

## Impact of alkalinity sources on the life-cycle energy efficiency of mineral carbonation technologies†

Abby Kirchofer,<sup>a</sup> Adam Brandt,<sup>\*b</sup> Samuel Krevor,<sup>c</sup> Valentina Prigiobbe<sup>d</sup> and Jennifer Wilcox<sup>b</sup>

Received 7th January 2012, Accepted 3rd July 2012

DOI: 10.1039/c2ee22180b

This study builds a holistic, transparent life cycle assessment model of a variety of aqueous mineral carbonation processes using a hybrid process model and economic input–output life cycle assessment approach (hybrid EIO-LCA). The model allows for the evaluation of the tradeoffs between different reaction enhancement processes while considering the larger lifecycle impacts on energy use and material consumption. A preliminary systematic investigation of the tradeoffs inherent in mineral carbonation processes is conducted to provide guidance for the optimization of the life-cycle energy efficiency of various proposed mineral carbonation processes. The life-cycle assessment of aqueous mineral carbonation suggests that a variety of alkalinity sources and process configurations are capable of net CO<sub>2</sub> reductions. The total CO<sub>2</sub> storage potential for the alkalinity sources considered in the U.S. ranges from 1.8% to 23.7% of U.S. CO<sub>2</sub> emissions, depending on the assumed availability of natural alkalinity sources and efficiency of the mineral carbonation processes.

### 1. Introduction

Mineral carbonation has been proposed as a technology to reduce greenhouse gas (GHG) emissions from fossil fuel combustion in a scalable manner.<sup>1</sup> In contrast to conventional

carbon dioxide capture and storage (CCS) systems where CO<sub>2</sub> is injected into the subsurface, mineral carbonation is an *ex situ* process where gaseous CO<sub>2</sub> is reacted with alkaline materials (such as silicate minerals and alkaline industrial wastes) and converted into stable and environmentally benign carbonate minerals. Mineral carbonation is based on chemical reactions that are analogous to the silicate weathering cycle responsible for CO<sub>2</sub> uptake on geologic time scales.<sup>2</sup> It utilizes input materials abundant worldwide and has the benefit of producing stable forms of CO<sub>2</sub>.

In addition, mineral carbonation products could find beneficial reuse. For example, mineral carbonation could be used to produce aggregates, fills and other bulk building materials, and some have argued that mineral carbonation products could partially offset Portland Cement consumption.<sup>3</sup> While the scale

<sup>a</sup>Program in Earth, Energy, and Environmental Sciences, Stanford University, 473 Via Ortega, Suite 140, Stanford, CA, 94305, USA

<sup>b</sup>Department of Energy Resources Engineering, Stanford University, 367 Panama Street, Stanford, CA, 94305, USA. E-mail: [abrandt@stanford.edu](mailto:abrandt@stanford.edu)

<sup>c</sup>Department of Earth Science and Engineering, Imperial College London, South Kensington Campus, SW7 2AZ, UK

<sup>d</sup>Petroleum and Geosystems Engineering, University of Texas at Austin, 1 University Station C0304, Austin, TX, 78712, USA

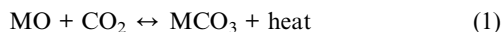
† Electronic supplementary information (ESI) available. See DOI: 10.1039/c2ee22180b

#### Broader context

Carbon dioxide (CO<sub>2</sub>) mineralization has been proposed as a mechanism to sequester CO<sub>2</sub>. Mineralization could be advantageous because it mimics silicate weathering cycles that remove CO<sub>2</sub> from the atmosphere over geologic time scales, and the CO<sub>2</sub> is therefore stored in very stable form. However, mineralization technologies are not well understood in many respects. One large uncertainty about mineralization technologies is the energy efficiency of mineralization pathways. If too much energy is consumed in mining, handling, processing, reacting, and disposing of mineralization materials, this large effort could result in more CO<sub>2</sub> emissions than the quantity of CO<sub>2</sub> sequestered, rendering mineralization ineffective as a storage mechanism. We build a process-model based life cycle assessment of mineralization technologies that allows comparison across a variety of mineralization feedstocks (*e.g.*, natural alkaline feedstocks and industrial byproducts) and technology specifications (*e.g.*, high vs. low temperature). Our model shows that there are some mineralization pathways that provide significant net CO<sub>2</sub> capture ability over the whole mineralization life cycle. This suggests that CO<sub>2</sub> mineralization should be explored as a CO<sub>2</sub> mitigation strategy, especially with extremely abundant natural mineral feedstocks.

of potential CO<sub>2</sub> sequestration in carbonate form far exceeds demand for potential beneficial reuses, such opportunities could improve the economics of early implementations of CO<sub>2</sub> capture processes.

Mineral carbonation refers to the reaction of CO<sub>2</sub> with alkaline divalent cations (*e.g.*, Ca<sup>2+</sup>, Mg<sup>2+</sup>, and Fe<sup>2+</sup>) to produce carbonate minerals that are stable at atmospheric conditions. A simplified general carbonation reaction is:



where MO is a metal oxide, M a divalent cation (*e.g.*, calcium (Ca<sup>2+</sup>) or magnesium (Mg<sup>2+</sup>)), and MCO<sub>3</sub> a carbonate product (*e.g.*, calcite (CaCO<sub>3</sub>) or magnesite (MgCO<sub>3</sub>)). Processes developed have focused mostly on performing these reactions in an aqueous medium, where CO<sub>2</sub> hydrolyzes to carbonic acid and metal oxides hydrolyze to basic components. Thus, the mineral carbonation process is a problem in acid–base chemistry<sup>4</sup> where the formation of carbonate products represents the neutralization of the acidic CO<sub>2</sub> with the basic (*i.e.*, alkaline) metal oxides and hydroxides. Acid–base neutralization processes are thermodynamically favored at atmospheric conditions, but a source of reactive alkalinity is required for the sequestration of the CO<sub>2</sub>.

Both natural and industrial alkalinity sources exist and have been investigated for mineral carbonation. Natural silicate minerals (*e.g.*, olivine, serpentine, and wollastonite) present an important potential feedstock resource for mineral carbonation because of their environmental abundance and widespread geographic availability.<sup>5</sup> For reasons of mineral availability, cation concentration, and reactivity, research on mineral carbonation has focused on the use of silicate minerals rich in Mg<sup>2+</sup> (*i.e.*, serpentine and olivine). In this case, the process consists of a dissolution step where silicate minerals release Mg<sup>2+</sup> into water and a precipitation step where Mg<sup>2+</sup> reacts with the aqueous carbonate species (CO<sub>3</sub><sup>2-</sup>) producing carbonate minerals. Although thermodynamic equilibria at atmospheric conditions favor the formation of carbonate minerals, reaction kinetics for silicate dissolution are very slow. Thus, natural silicates do not represent a particularly reactive source of alkalinity and elevated temperature and pressure or the use of chemical additives is required to perform the conversion on time scales relevant to industrial CO<sub>2</sub> emission.<sup>6–8</sup>

In comparison, industrial by-products tend to be more reactive than silicate minerals, but their use is limited by their production rates. Cement kiln dust (CKD),<sup>9,10</sup> coal fly ash (FA),<sup>6</sup> and steel-making slag (SS)<sup>11–14</sup> are the most promising industrial alkaline by-products given their relative abundance and demonstrated carbonation capacity. Despite the attractive reactivity of industrial by-products, the production rate is small compared to the scale of CO<sub>2</sub> emissions.<sup>15</sup> Nonetheless, they might serve as low-cost alkalinity sources for the development of mineral carbonation technologies, which could be extended to the abundant but more expensive natural alkalinity sources such as silicate minerals.

Drawbacks to mineral carbonation include significant materials handling requirements and potentially high energy consumption.<sup>1</sup> Because the scale of CO<sub>2</sub> production is so large, mineral carbonation would require large amount of materials in order to sequester a significant quantity of CO<sub>2</sub>. The energy

demands of carbonation include grinding, heating, mixing, and transport of feedstocks and products and may result in emissions of CO<sub>2</sub> large enough to challenge the benefits of this sequestration process.

The success of mineral carbonation depends critically on the cost and efficiency with which alkalinity can be extracted from feedstocks, and subsequently carbonated. If an energy efficient, scalable process for alkalinity extraction or generation exists, then mineral carbonation will be effective; otherwise mineral carbonation is likely to be costly per tonne of CO<sub>2</sub> mitigated, and could even be a net CO<sub>2</sub> source instead of a sink. For both industrial and natural alkalinity sources, various process schemes have been developed to enhance reaction kinetics, such as heat-pretreatment, mineral pulverization, and the optimization of reaction conditions.<sup>6,16,17</sup> However, to date, this technology is still associated with high-energy costs because of the mining and pre-processing (*e.g.*, grinding) required, especially for natural alkalinity sources, and the large materials throughput.<sup>6</sup>

Previous studies have identified process conditions optimal for enhancing the carbonation reaction kinetics (in particular regarding the dissolution step).<sup>6,14,18</sup> No study, however, has yet performed a scheme that optimizes these conditions with the goal of producing an energetically viable carbonation process. In this study we seek to evaluate the tradeoffs in using various reaction enhancement process schemes in the context of the life cycle energy use and material consumption. In the current work, capital costs are only included in order to evaluate energy and material consumption; future work should include the investigation of capital expenditures (CAPEX). This study builds a holistic, transparent life cycle assessment model of a variety of aqueous mineral carbonation processes using a hybrid process model and economic input–output life cycle assessment approach (hybrid EIO-LCA). A preliminary systematic investigation of the tradeoffs inherent in mineral carbonation processes can provide guidance for the optimization of the life-cycle energy efficiency of various proposed mineral carbonation processes.

## 2. Methods

### 2.1 LCA model

The goal of our LCA tool is to compare the energy efficiency and net CO<sub>2</sub> storage potential of a variety of aqueous mineral carbonation processes on a consistent basis by determining the energy and material inputs associated with each implementation. Our model relies on the peer-reviewed scientific literature and the patent literature.<sup>12,19–21</sup> The model assumes input of pure compressed CO<sub>2</sub> (*i.e.* separation and compression are outside the system boundaries), so the processes modelled should be considered as a form of CO<sub>2</sub> storage. The important variables contributing to the overall lifecycle assessment are: (1) the extent of reaction for feedstock minerals, (2) the extent of grinding to reduce the average particle size of feedstocks, (3) the residence time of materials in a reactor, (4) the number of reactors required for a given throughput, and (5) the conditions at which the reactions are performed. All main process stages are included in the tool, and comprehensive system boundaries are applied throughout the model. Because our tool aims to compare

processes that vary significantly in input resource and process design, the model is built at a general, first-order level.

The model uses a hybrid process model and economic input–output life cycle assessment approach (hybrid EIO-LCA). This methodology accounts for the following three types of energy consumption: on-site energy consumption, energy of material and energy inputs consumed in the sector of interest (embodied direct energy), and energy of material and energy inputs consumed in all other sectors (embodied indirect energy). Including both on-site and embodied energy allows a full accounting of the total greenhouse gas (GHG) reduction benefits of each process scheme. The functional unit for the model is mineral carbonation of 1000 ton per day (t per day) of CO<sub>2</sub>.

The process-model core of the mineral carbonation LCA tool includes eight process stages (see Scheme 1). These process stages are defined generically to be applicable to a variety of mineral carbonation technologies:

1. Extraction – Mining of natural alkalinity source or separation and selection of the industrial alkalinity source;
2. Transport – Movement of unprocessed alkalinity source to processing site;
3. Physical preprocessing – Physical treatment of alkalinity source, including crushing or grinding;
4. Chemical conversion – Reaction of CO<sub>2</sub> with alkalinity source to form stable mineral. This process stage might consist of two parts if natural alkalinity sources are used, *i.e.*, a dissolution step and a precipitation step.
5. Post-reaction processing – Processing required after the carbonation reaction;
6. Transport – Transport of produced minerals to disposal or beneficial reuse site;

7. Beneficial reuse – Reuse of product in place of other previously used compound;

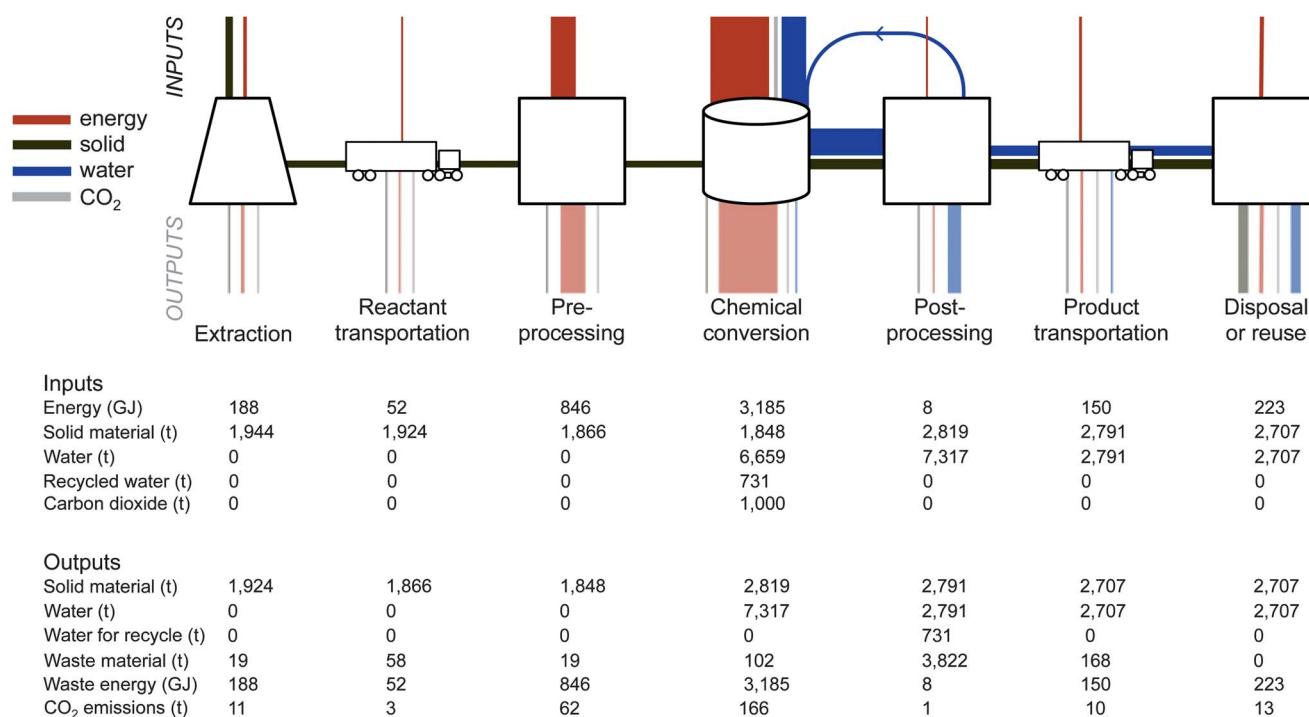
8. Disposal – Placement of mineral matter in disposal site for long-term storage.

Each of these stages is modeled using physical and chemical principles, described in detail below.

The total (on-site plus embodied) energy consumption is calculated using the EIO-LCA tool from Carnegie Mellon University to convert the direct consumption of energy, materials, and services into life cycle energy consumption [2002 U.S. model].<sup>22</sup> EIO-LCA results provide total energy consumed (within a North American Industry Classification System [NAICS] sector and for all other sectors) per dollar of economic activity occurring in a given sector. These EIO-LCA results are used to generate direct (within-sector) and indirect (all other sectors) energy consumption, as detailed in the ESI. Consumption per unit of economic activity is then converted to consumption per physical unit using commodity price indices (*e.g.*, \$ MJ<sup>-1</sup> natural gas or \$ t<sup>-1</sup> of steel).

## 2.2 Process modeling

**Extraction.** The extraction process stage includes mining, grinding, and loading of alkalinity sources into the transport system. The amount of alkalinity source extracted is determined based on the mineral carbonation rate of 1000 t CO<sub>2</sub> per day, the mass ratio of alkalinity source to CO<sub>2</sub>, the estimated extent reacted of the alkalinity source, and the reaction efficiency. Material losses of 1% are assumed for this stage (*e.g.*, mass output is 1% less than mass treated). To model the energy consumption of extraction, it is assumed that the mining of



**Scheme 1** Life cycle process model schematic for aqueous mineral carbonation of 1000 t CO<sub>2</sub> based on olivine – 155 °C case; thickness of lines is scaled to the energy and mass fluxes (inputs enter from top, outputs leave through bottom).

alkalinity sources can be represented by low or high intensity extraction. The collection and handling of industrial alkalinity sources (*i.e.*, CKD, FA, SS) is assumed to consume 50% of the energy of low intensity extraction. The energy consumption calculations are based on stone mining (NAICS 212310; 48.8 MJ t<sup>-1</sup> direct, 97.0 MJ t<sup>-1</sup> total) for low intensity and sand/gravel mining (NAICS 212320; 192.9 MJ t<sup>-1</sup> direct, 360.9 MJ t<sup>-1</sup> total) for high intensity mining. Economic to physical scaling is based on USGS commodity price indexes.<sup>23,24</sup>

**Transport.** The transport process stages include the transport of alkalinity sources from the extraction site to the processing site and from the post-reaction processing site to the beneficial reuse or disposal site. Transport is assumed to be by truck for distances less than 100 km, and by rail for distances 100 km and above. Energy use is assumed to be proportional to tonnes of material moved, and material losses of 3% in transport are assumed. Energy consumption calculations are based on rail freight (NAICS 482000; 0.206 MJ t<sup>-1</sup> km<sup>-1</sup> direct, 0.270 MJ t<sup>-1</sup> km<sup>-1</sup> total). For comparison to EIO-LCA results, energy values were also calculated based on 2007 statistics of total mass-distance traveled and total diesel consumed.<sup>25</sup> For these comparison calculations, it was assumed that transport energy requirements for alkalinity sources equal the average for the U.S. freight industry, and capital investment in rail lines and embodied energy in rail transport equipment, loading equipment, and transfer stations were neglected. The direct energy (diesel) consumed per mass-distance (t-km) obtained was 0.231 MJ t<sup>-1</sup> km<sup>-1</sup>, which is close to the EIO-LCA results of 0.225 MJ t<sup>-1</sup> km<sup>-1</sup> petroleum and 0.270 MJ t<sup>-1</sup> km<sup>-1</sup> total energy consumed.

**Physical preprocessing.** The physical preprocessing stage models the grinding required to reduce the particle size of the alkalinity source. All energy for grinding is assumed to be electricity, capital investments are assumed to equal those of the chemical conversion stage with type (a) reactors used (described below), and material losses of 1% are assumed. The energy required for grinding a particular feed,  $E_G$ , is calculated as a function of the 80% passing sizes of the final product,  $P$ , and initial feed,  $F$ , in microns ( $\mu\text{m}$ ), according to:

$$E_G = 10W_i \left( \frac{1}{P^{0.5}} - \frac{1}{F^{0.5}} \right) \quad (2)$$

with  $W_i$  equal to Bond's work index for the material.<sup>26</sup> ESI provides the Bond work indices for the alkalinity sources investigated. Input particle size is assumed to be 1 cm (10 000  $\mu\text{m}$ ), and the output particle size is a reaction parameter ranging from 4 to 2000  $\mu\text{m}$ . For the total energy calculations, the embodied energy of electricity is included to account for indirect energy consumption, based on power generation (NAICS 221100).

**Chemical conversion (dissolution and precipitation reactions).** The chemical conversion stage requires heating and mixing of reactants during the dissolution and carbonation reactions and the consumption of materials during the reaction (*e.g.*, cement and steel during the construction of the reactor, water during its operation). The masses of reactants (*e.g.*, alkalinity source, water) required to carbonate CO<sub>2</sub> at a rate of 1 t per day are determined based on the stoichiometry of the carbonation

reaction and the assumed reaction efficiency. Material losses of 1% are assumed during the precipitation reaction.

**Reactor tanks.** Energy consumption due to the construction of the reactor tanks is assumed to equal the embodied energy of the cement and steel consumed due to tank use. The steel and cement consumed for the reactor tanks has been evaluated for two types of generic stainless steel reactor tanks: (a) cylindrical tank with flat ends for low  $P$  processes (with  $P \leq 1$  bar), (b) cylindrical tank with semi-ellipsoidal caps for high  $P$  processes ( $P$  up to 100 bar). The tank wall thickness is calculated for each tank type, as detailed below. For tank types (a) and (b) the mass of steel required per tank is calculated based on the tank wall thickness and dimensions, and the mass of cement required (t per day) is assumed to equal the mass of steel. The minimum wall thickness,  $T_T$  (mm), is calculated according to:

$$T_T = \frac{\rho_L H_L g D}{2SE \times 10^3} \quad (3)$$

with  $\rho_L$  equal to the liquid density (kg m<sup>-3</sup>),  $H_L$  the liquid depth (m),  $g$  the gravitational acceleration (m s<sup>-2</sup>),  $D$  the tank diameter (m),  $S$  the maximum allowable stress for the tank material ( $N \text{ mm}^{-2}$ ), and  $E$  the joint efficiency.<sup>27</sup> Due to the abrasive nature of mineral carbonation, this value is conservatively increased by the greater of 2 mm or 10%. Tank type (a) has 10 m diameter and height, 6.8 mm wall thickness, 785 m<sup>3</sup> volume, and a required mass of steel ~26 t per tank. Tank type (b) has 2 m diameter, 10 m height, 101.6 mm wall thickness, 27 m<sup>3</sup> volume, and a required mass of steel ~56 t per tank.

Tank life is assumed to equal 20 years (7300 days), and the mass of steel or cement consumed (t per day) due to tank use is calculated by dividing the mass per tank (t per tank) by the assumed life of the tank (day per tank). The number of tanks required is calculated by dividing the volume of reactor space required (m<sup>3</sup>) by the volume per reactor tank (m<sup>3</sup>).

To account for other capital investment (*e.g.*, tank insulation materials, pipes, conveyors, pumps, and other equipment) embodied energy from tanks is multiplied by a factor of 1.3. The resulting calculations show that embodied emissions in capital investment is a negligible fraction of overall emissions (<2% in the optimized olivine case), therefore, further detailed design of the facility is not required.

**Water consumption.** The water consumption is defined as the water demand (t per day) less the input rate of recycled water (t per day) from the downstream process stages. The energy consumption due to fresh water is based on water supply (NAICS 221100; 0 MJ t<sup>-1</sup> direct, 4.66 0 MJ t<sup>-1</sup> total).

**Heating.** The energy consumption for heating is assumed to equal the energy consumed to heat reaction materials to the reaction temperature, and the energy consumed to maintain such a temperature accounting for heat loss from reactor tanks. The energy source for heating is assumed to be natural gas. The energy required for heating a particular material,  $E_H$ , is calculated as a function of the mass of the material heated,  $m$  (t), the specific heat capacity of the material,  $C_P$ , and the difference between the input temperature and the reaction temperature,  $\Delta T$ , according to:

$$E_H = mC_p\Delta T. \quad (4)$$

Input temperatures for fresh water and alkalinity sources are assumed to equal 10 °C and 20 °C, respectively. Recycled water input temperature is assumed to equal the reaction temperature less 33% heat loss during post-reaction processing and feedback (this assumption is varied in the sensitivity analysis). ESI provides the heat capacity and heat of reaction used for various reaction materials. The external heat required is decreased by the heat released during the reaction process. These heats of reaction amount to 1.00 MJ kg<sup>-1</sup> for olivine (100% reacted) and 0.27 MJ kg<sup>-1</sup> for serpentine. This heat of reaction provides up to 100% of the heat requirements of carbonation, greatly lessening the need for external energy inputs.

The energy required to maintain reactor (and reaction mixture) temperatures is assumed to equal to the energy loss from tanks due to heat loss. Heat loss from reactor tanks is calculated assuming the tanks are stainless steel cylinders insulated with 5 cm mineral fiber reinforced with aluminum foil. ESI provides the thermal conductivity,  $k$ , and emissivity,  $\epsilon$ , for tank materials.<sup>28</sup> It is assumed that the heat flux from the tank,  $\phi_q$  (W m<sup>-2</sup>), must equal heat flux to the surrounding environment due to convection and radiation, which is calculated according to:

$$\Phi_q = h(T_O - T_A) + \epsilon_1\sigma(T_O^4 - T_A^4) \quad (5)$$

with  $T_O$  representing the outside temperature of the tank and  $T_A$  representing the ambient temperature of the surrounding environment. The temperature on the outside of the tank,  $T_O$ , is determined by assuming heat flux through the tank due to conduction wall must equal heat flux to the surrounding environment due to convection and radiation.  $T_O$  is calculated according to:

$$\frac{(T_R - T_O)}{r_1 \times \frac{\ln(r_O/r_S)}{k_I} \times \frac{\ln(r_S/r_1)}{k_A}} = h(T_O - T_A) + \epsilon_1\sigma(T_O^4 - T_A^4) \quad (6)$$

(taking the physically meaningful root as  $T_O$ ), with  $T_R$  defined as the temperature of the reaction;  $r_1$  the inner tank radius,  $r_O$  the outer tank radius, and  $r_S$  the non-insulated tank radius (*i.e.*, outer radius of the stainless steel tank);  $k_I$  and  $k_A$  defined as the thermal conductivity of insulation and steel (W m<sup>-1</sup> K<sup>-1</sup>), respectively; the convection coefficient,  $h$ , assumed to equal 20 W m<sup>-2</sup> K<sup>-1</sup>;  $\epsilon_1$  defined as the emissivity of insulation; and the Stefan-Boltzman constant,  $\sigma$ .<sup>28</sup>

**Mixing.** Energy consumed by mixing reactants is determined based on the power required to mix a certain volume of reactant mixture. It is assumed that mixing is by electricity-powered vertical flat-blade turbines, CO<sub>2</sub> is injected at the bottom of the turbine shaft, and flow is turbulent.<sup>29</sup> ESI provides further description of mass transfer of CO<sub>2</sub> in the reactor system. Mixing power,  $P_M$  (kW), is calculated according to:

$$P_M = N_p\rho N^3 D^5 \quad (7)$$

with  $N_p$  defined as the power number, equal to 3.75;  $\rho$  the mixture density;  $N$  the impeller speed, equal to 0.6 rps; and  $D$  the impeller

diameter, assumed to equal 1/3 the tank diameter.<sup>29,30</sup> Given the assumed mixing design, the flow in the reaction vessels is fully turbulent and CO<sub>2</sub> is well-dispersed throughout the system.

**Post-reaction processing.** Post-reaction processing includes treatment of the carbonation reaction product to separate water and solids by clarifier, liquid cyclone, and/or centrifugal separation. It is assumed that separation processes are powered by electricity, that capital investment equals that of the chemical conversion stage type (a) reactors used, and that material losses equal 5% during post-reaction processing. The type of separation process used is based on the product mixture and the primary goal of the processing (*e.g.*, to produce clarified water for reuse in the chemical conversion stage, or to produce dry carbonate material), and multiple processes may be used in series.

**Clarifier.** The clarifier process is used to clarify 75–80 vol.% water from a feed mixture with 0.1–35 wt% solids. Clarifier tank diameters typically range from 2–200 m, and heights from 2.5–3.5 m. The power consumed,  $P_C$  (kW), is a function of the tank diameter,  $D$ :

$$P_C = c_C D^2 \quad (8)$$

with the coefficient  $c_C$  ranging from 0.003–0.006. For this model, the coefficient and diameter are assumed to be 0.0045 and 25 m, respectively. It is assumed that the clarified output water may be recycled as input water to the carbonation reaction without additional processing. The energy and separation data for the clarifier process, as well as for the liquid cyclone and centrifugal filter separation processes, are based on averages given by Ulrich and Vasudevan, 2004, and are provided in ESI.<sup>31</sup>

**Liquid cyclone.** The liquid cyclone process is used to produce 30–50 wt% solid mixture from a feed mixture with 4–35 wt% solids. Cyclone tank diameters typically range from 0.01–1 m, and heights from 0.3–3 m. The power consumed,  $P_C$  (kW), is a function of the volumetric flow rate,  $q_V$  (m<sup>3</sup> s<sup>-1</sup>):

$$P_C = c_C q_V \quad (9)$$

with the coefficient  $c_C$  ranging from 100–300. For this model, the coefficient and volumetric flow rate are assumed to be 200 and 0.075 m<sup>3</sup> s<sup>-1</sup>, respectively.

**Centrifugal filter.** The centrifugal filter process is used to produce 80–95 wt% solid mixture from a feed mixture with 30–60 wt% solids. Centrifugal filter tank diameters typically range from 0.2–1.4 m, and heights from 0.5–2 m. The power consumed,  $P_C$  (kW), is a function of the solids input rate,  $q_M$  (kg s<sup>-1</sup>):

$$P_C = c_C q_M \quad (10)$$

with the coefficient  $c_C$  ranging from 3–30 and  $q_M$  from 0.002–0.15 kg s<sup>-1</sup>. For this model, the coefficient and volumetric flow rate are assumed to be 16.5 and 0.076 m<sup>3</sup> s<sup>-1</sup>, respectively.

**Beneficial reuse.** The beneficial reuse stage accounts for the displacement of aggregate with the carbonation product. We use

life cycle energy intensity from the EIO-LCA tool for the medium intensity mined product (crushed limestone) as an analog to embodied energy in aggregate. This value of  $-97 \text{ MJ t}^{-1}$  ( $4.5 \text{ kg CO}_2 \text{ t}^{-1}$ ) co-production credit aligns well with data on energy consumption for aggregate from Horvath (2004), which calculates  $115 \text{ MJ t}^{-1}$  for crushed stone.<sup>32</sup> It is assumed that no additional capital investment is required to perform beneficial reuse (e.g., the construction industry will already have trucks for hauling aggregate). It is assumed that the carbonate product must be 90% solid for re-use, and thus all cases with beneficial reuse require solid-liquid separations using the centrifugal filter, described above. Re-use of carbonation products in chemical markets was not considered feasible because the potential scale of production from mineral carbonation is much greater than that of existing chemical markets.<sup>33</sup>

**Disposal.** The disposal stage accounts for the energy burden of final disposal of carbonation products that are not reused (e.g., landfilling, aqueous disposal). For solid products not beneficially reused, it is assumed that the material will be disposed as mine backfill, and that backfill requires 50% of the low energy intensity of mining.

### 2.3 Mineral carbonation reaction modeling

The LCA model includes mineral carbonation pathways associated with alkalinity sourced from both industrial by-products and natural silicate minerals. Aqueous mineral carbonation processes have been developed for both. The aqueous processes involve two steps (sometimes simultaneously occurring within the same reactor), dissolution of cations from the silicate minerals into solution followed by nucleation and growth of carbonate precipitate.<sup>16,34–36</sup> In the approach used in this study, reaction kinetics and extent of reaction are taken to be independent of the partial pressure of  $\text{CO}_2$ . This is based on the assumption that  $\text{CO}_2$  will be delivered at supercritical pressures (9–10 MPa) where transportation is most cost-effective (see Chapter 4 of IPCC, 2005).<sup>3</sup> Different reaction modeling approaches are used to treat industrial by-products and natural silicate minerals, due to the

difference in reaction kinetics for each category of alkalinity source, as described in the following sections.

**Industrial by-products.** Industrial by-products tend to have a mixture of oxides (e.g.,  $\text{CaO}$  and  $\text{MgO}$ ) and silicates; while oxides dissolve readily in solution and react readily with  $\text{CO}_2$ , silicates require a dissolution step to release the cations available for carbonation. Given the complex and varied chemophysical properties of industrial by-products, there is no general reaction model to determine the extent of their reaction; rather, data from the literature are for specific reaction conditions and alkalinity source compositions. Therefore, the extent of the reaction is based on experimental data from the literature for CKD,<sup>9</sup> FA,<sup>37</sup> and SS,<sup>12</sup> the industrial by-products considered in this work.

**Natural silicates.** Due to the low reactivity of natural silicate (such as serpentine and olivine), their carbonation requires an aqueous process consisting of a dissolution step where cations are released into solution followed by a precipitation step where carbonate minerals are formed upon reaction of the cations with the dissolved  $\text{CO}_2$ . These two steps might be performed in a single- or two-stage process. As silicate dissolution is the rate-limiting step, we analyze the extent of this reaction more extensively and investigate the effect of temperature, solution composition, particle size, and residence time, assuming a solution with constant  $\text{pH} = 6$ . This  $\text{pH}$  is easily supported by  $\text{CO}_2$  partial pressures from atmospheric to 9 MPa (approximate transport pressure), and we assume that the  $\text{pH}$  can be fixed through management of the  $\text{CO}_2$  pressure over the system at negligible energy penalty. We described the temporal evolution of the particle size distribution of a polydisperse olivine suspension using the population balance equation (PBE) coupled with a mass balance equation of olivine and assuming a dissolution rate equation reported in Hänchen *et al.* (2006).<sup>7,38–41</sup> We assumed that all dissolved cations react with  $\text{CO}_2$  during the precipitation stage to form carbonate (i.e., 100% of the dissolution-step extent reacted reacts with  $\text{CO}_2$ ).

Informal optimization of the aqueous mineral carbonation processes for a given alkalinity source is performed by

**Table 1** Values of the reaction parameters used in each case. Extent reacted is defined as the fraction of alkalinity source that reacts with  $\text{CO}_2$  to form carbonate. In all cases a reaction efficiency of 90% is assumed and separations included clarifier/thickener and liquid cyclone, except for the CKD – 25 °C case, which was optimized with no separation process

	Net $\text{CO}_2$ avoided (t per day)	Extraction particle size ( $\mu\text{m}$ )	Percent solid (wt%)	$\text{CO}_2$ pressure (bar)	Temperature (°C)	Reaction particle size ( $\mu\text{m}$ )	Residence time (min)	Reactor volume ( $\text{m}^3$ )	Reactor tanks <sup>a</sup> (type, unit)	Extent reacted ( $\text{t t}^{-1}$ )
Ol – 25 °C	–17 782	10 000	20	90	25	4	1440	795 699	(b) 29 607	0.01
Ol – 105 °C	586	10 000	20	90	105	4	1440	14 368	(b) 535	0.59
Ol – 155 °C	733	10 000	20	90	155	10	1440	8827	(b) 328	1.00
Ol – reuse <sup>b</sup>	747	10 000	20	90	155	10	1440	8827	(b) 328	1.00
Se – 155 °C	346	10 000	20	90	155	4	1440	15 110	(b) 562	0.71
CKD – 25 °C	858	28	54	0.8	25	28	432	3505	(a) 4	0.52
CKD – reuse <sup>b</sup>	854	28	54	0.8	25	28	432	3505	(a) 4	0.52
FA – 25 °C	552	100	5	0.1	25	100	270	30 721	(a) 39	0.45
FA – 75 °C	449	100	5	0.1	75	100	270	17 775	(a) 23	0.78
SS – 25 °C	656	16 000	9	1	25	100	30	2800	(a) 4	0.36
SS – 100 °C	39	16 000	9	1	100	100	30	2120	(a) 3	0.47

<sup>a</sup> Tank type (b) used for high  $P$  processes, see reactor tank section for details. <sup>b</sup> Reuse = beneficial reuse of carbonate product, considered for the Ol – 155 °C and CKD – 25 °C cases.

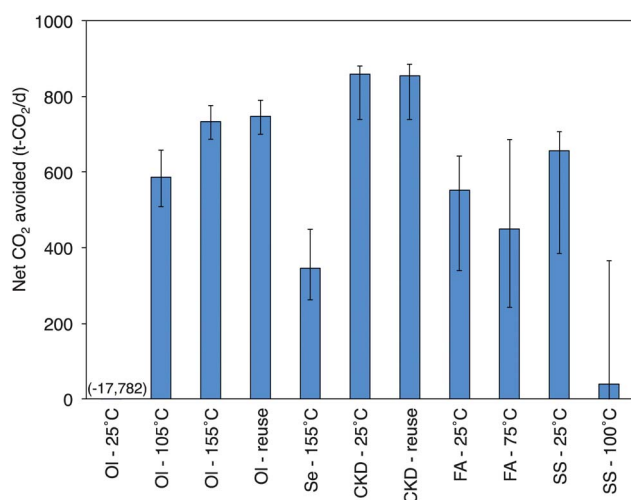


**Fig. 1** Comparison of cases; error bars are sourced from process efficiency ranges; Ol = olivine, Se = serpentine.

systematically varying the model input parameters (*i.e.*, process variables and reaction conditions) across a range of process model parameters suggested by the literature and based on a) parameter values tested in the dissolution model (for olivine and serpentine), or b) data available in the literature (for CKD, FA, and SS).

In order to evaluate model uncertainty, process efficiency ranges are explored based on values from literature or reasonable ranges of assumption. The efficiency assumptions used to estimate the uncertainty in the results are described in the ESI.

### 3. Results and discussion

The net CO<sub>2</sub> storage potential of aqueous mineral carbonation is evaluated for olivine, serpentine, CKD, FA, and SS across a range of reaction conditions and process parameters. In the following discussion, a handful of representative cases will be considered to exemplify the results and highlight key findings. For the select cases, the reaction parameters are summarized in Table 1, and the net CO<sub>2</sub> avoided (t-CO<sub>2</sub> per day) is shown in Fig. 1. The net CO<sub>2</sub> avoided is defined as the total CO<sub>2</sub> sequestered (1000 t per day) less life-cycle CO<sub>2</sub> emissions. For each case, the parameters are selected to optimize the process for given alkalinity source and temperature.

#### 3.1 Natural silicate alkalinity sources – olivine

Several cases for olivine are highlighted below: ambient temperature (25 °C), medium temperature (105 °C), and high temperature (155 °C). For the cases tested, a minimum net CO<sub>2</sub> emissions of -733 t-CO<sub>2</sub> per day occurs with the high temperature case. Net CO<sub>2</sub> emissions for the low and medium temperature cases are 17 782 t-CO<sub>2</sub> per day and -586 t-CO<sub>2</sub> per day, respectively. For Ol - 25 °C and Ol - 105 °C, the optimal particle size is 4 μm, while for Ol - 155 °C 10 μm is optimal. Fig. 2 provides the CO<sub>2</sub> emissions per process stage for the ambient and high temperature cases. In comparison to the 155 °C case, the 25 °C case requires over 80 times more olivine and water per 1000 t-CO<sub>2</sub> mineralized, due to the low reactivity of olivine at

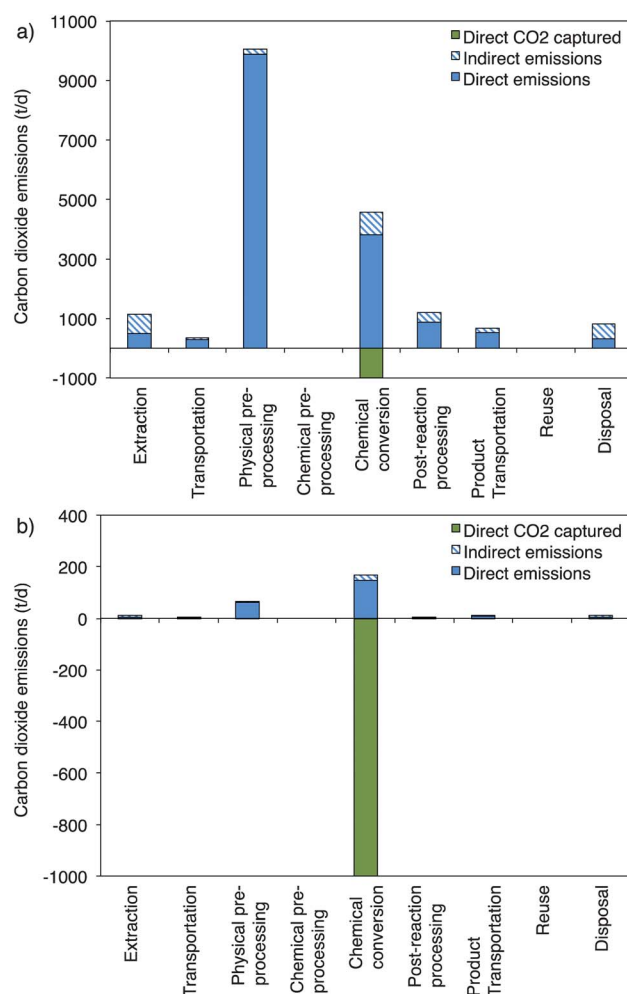


**Fig. 2** CO<sub>2</sub> emissions of the mineral carbonation process using olivine as an alkalinity source. (a) 25 °C, (b) 155 °C.

ambient temperature; this results in 59 times the energy consumption throughout the entire process due to the higher mass throughput.

Overall, net CO<sub>2</sub> emissions are minimized (*i.e.*, net storage is maximized) by increasing alkalinity source reactivity and decreasing the amount of alkalinity source and water processed per ton of CO<sub>2</sub> mineralized. As such, any measure which increases the extent reacted tends to improve the overall life-cycle energy efficiency. Increasing temperature, decreasing particle size, and increasing residence time maximize extent reacted dramatically and improve the life-cycle energy efficiency and the net mitigation potential of the process, as shown in Fig. 3 (next page). Increasing the residence time decreases the process efficiency more than increasing temperature or decreasing particle size. Increasing residence time is costly because it equates to increasing the amount of material processed at any given time, and therefore increases the amount of mixing and heating required during the chemical conversion stage.

In all cases, enhancement measures improve the net mitigation potential only insofar as they increase the extent reacted—once 100% extent reacted is attained, additional energy expenditure in enhancement measures (*e.g.*, increase in residence time, increase

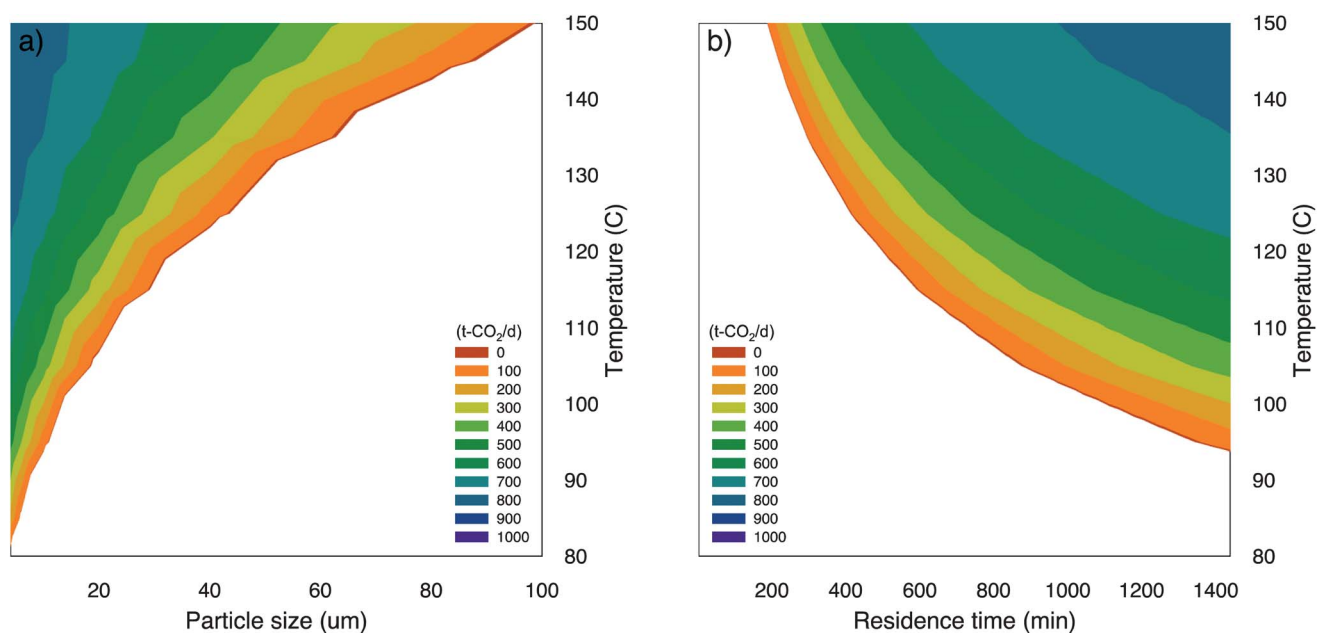


**Fig. 3** Net mitigation potential for 1000 t CO<sub>2</sub> per day gross capture capacity facility. Net capture rate is presented as a function of (a) particle size and temperature (residence time = 1440 min) and (b) residence time and temperature (particle size = 10 μm); white represents negative mitigation potential (e.g., life cycle emissions exceed 1000 t CO<sub>2</sub> per day and therefore negate benefit of mineral carbonation).

in temperature, or decrease in particle size) serves no purpose but to decrease the process efficiency. By improving olivine's reactivity, such measures allow for residence time to decrease while

still attaining 100% extent reacted. For instance, for the OI - 155 °C case, the optimized particle size is 10 μm (the largest particle size at which 100% extent reacted is attained), while for

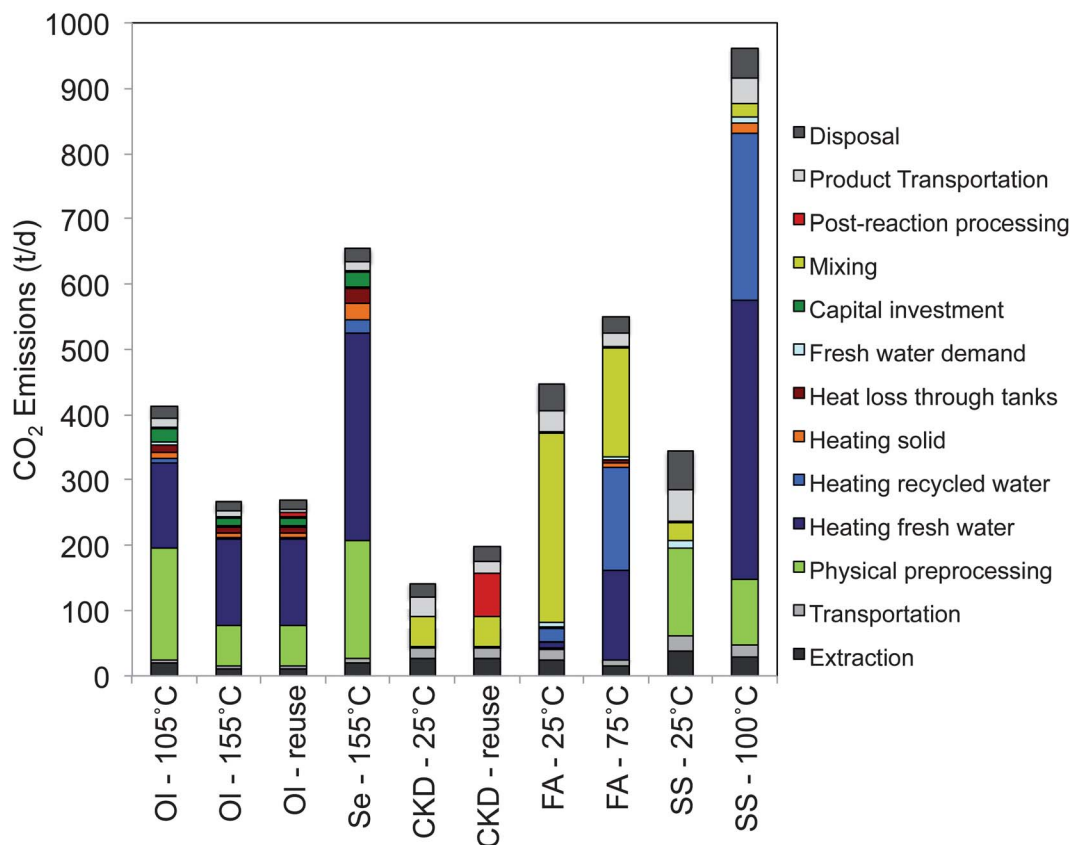


**Fig. 4** CO<sub>2</sub> emissions per 1000 t-CO<sub>2</sub> per day sequestered for the mineral carbonation processes with net CO<sub>2</sub> mitigation potential.



the 105 °C and 25 °C cases it is 4 μm (the minimum particle size investigated), and 100% extent reacted is not attained. As Fig. 3 (next page) shows, olivine mineral carbonation processes are only feasible for high *T*, small particle size, and long residence times. Based on current results, the efficiency of an optimized olivine-based mineral carbonation process can reach 73%.

### 3.2 Natural silicate alkalinity sources – serpentine

For serpentine cases, the maximum efficiency of 346 t-CO<sub>2</sub> per day was obtained at 155 °C and 4 μm; this corresponds to 71% extent reacted. The life-cycle energy efficiency of a serpentine-based mineral carbonation process is in general lower than that of an olivine-based process, because the dissolution kinetics of serpentine are slower than those of olivine.

### 3.3 Industrial by-product alkalinity sources

For the CKD, FA, and SS cases evaluated, a minimum net CO<sub>2</sub> emissions of –858 t-CO<sub>2</sub> per day occurs with the CKD – 25 °C case. Net CO<sub>2</sub> emissions for the best FA and SS cases are –552 t-CO<sub>2</sub> per day and –656 t-CO<sub>2</sub> per day, respectively. It is important to consider that the parameters used in the industrial by-product cases were based on experimental data from the literature, and as such the results were not optimized as they were for olivine and serpentine. Furthermore, the percent solids varied widely between the experiments surveyed, with CKD at 54%, FA at 5%, and SS at 9%. It is expected that FA and SS results would be greatly improved by increasing the percent solids, which would decrease the heating, mixing, water consumption, and separations energy requirements.

Fig. 4 shows the contribution to CO<sub>2</sub> emissions for the mineral carbonation processes with net CO<sub>2</sub> mitigation potential. Overall, the major energy drivers are heating, mixing for the industrial by-products (which use the larger tank type (a)), and grinding (in the cases where requiring grinding); these processes are related by the material residence time in the reactor and the overall mass throughput. For natural silicates (which use tank type (b)) energy consumed due to capital investment is also significant. A comparison of the relative efficiency between the high and low temperature cases for olivine, FA, and SS reveals the different role temperature plays in life-cycle energy efficiency for the various alkalinity sources. In general, increasing the temperature dramatically improves the overall efficiency of olivine carbonation processes because higher temperatures increase olivine's extent reacted. For FA, whose extent reacted is less dependent on temperature, the total net CO<sub>2</sub> mitigation potential is approximately 20% greater for the 25 °C case than for the 75 °C case. As Fig. 4 shows, the distribution of energy demand (and, therefore, CO<sub>2</sub> emissions) between and within the various process stages is quite different, highlighting the tradeoff between the additional reactivity gained with heating, which leads to less material processed (*e.g.*, mixed during the reaction stage) per CO<sub>2</sub> captured, and the increase in energy consumption and CO<sub>2</sub> emissions due to heating.

For FA, mixing accounts for the vast majority of CO<sub>2</sub> emissions in the low temperature case, while in the high temperature case both mixing and heating account for the majority of CO<sub>2</sub> emissions. In the case of SS, because higher temperatures do not

improve the reactivity of SS, increasing the temperature tends to worsen the efficiency of SS carbonation processes. For the 25 °C case, mixing accounts for 69% of CO<sub>2</sub> emitted during the chemical conversion stage, while in the 100 °C case, materials heating accounts for 96% of CO<sub>2</sub> emitted.

### 3.4 Beneficial re-use

To investigate the net impact of beneficial re-use of the carbonate product on the life-cycle energy efficiency of a mineral carbonation process, the optimum silicate and industrial by-product cases, *i.e.*, OI – 155 °C and CKD – 25 °C, were implemented assuming 100% re-use of the carbonate product as aggregate. For re-use, there is a tradeoff between the gain in efficiency due to the mitigation credit for replacing aggregate, and the loss in efficiency due to the greater processing of the carbonate products required prior to reuse. As Fig. 4 shows, both the OI – reuse and CKD – reuse cases resulted in greater post-reaction processing CO<sub>2</sub> emissions, due to the additional drying steps. In the case of olivine, slightly more CO<sub>2</sub> emissions are mitigated by replacing aggregate with the carbonate products, and the overall life-cycle efficiency improves by 14 t-CO<sub>2</sub> per day for olivine; however, for CKD reuse decreases the life-cycle efficiency by 4 t-CO<sub>2</sub> per day.

### 3.5 Model sensitivity

To investigate the relative effect of reaction and process parameters, select parameters were varied independently and the net CO<sub>2</sub> mitigation of case was compared to the base high temperature olivine case OI – 155 °C. Fig. 5 displays the parameter dependence of the net CO<sub>2</sub> mitigation for % water recycled, used reaction exothermicity, recycled water heat loss, reaction efficiency, mixing speed, extraction particle size, product transport, reactant transport, capital cost, and material losses. As Fig. 5 shows, the assumed reaction efficiency and amount of water recycled impact the net CO<sub>2</sub> mitigation most significantly. Used reaction exothermicity and product transport distances also significantly impact the net CO<sub>2</sub> mitigation.

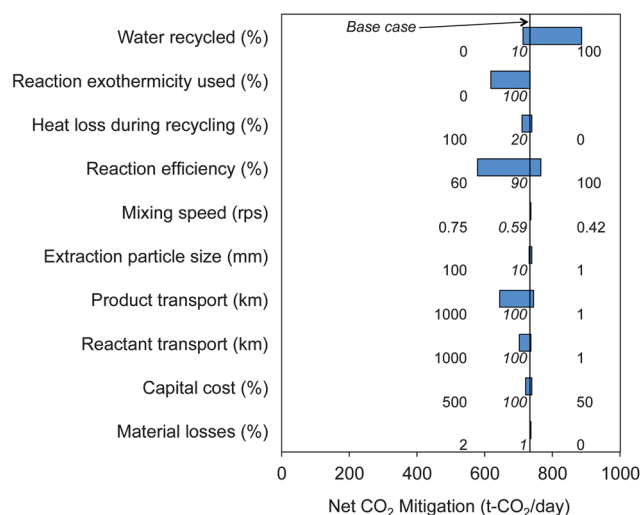
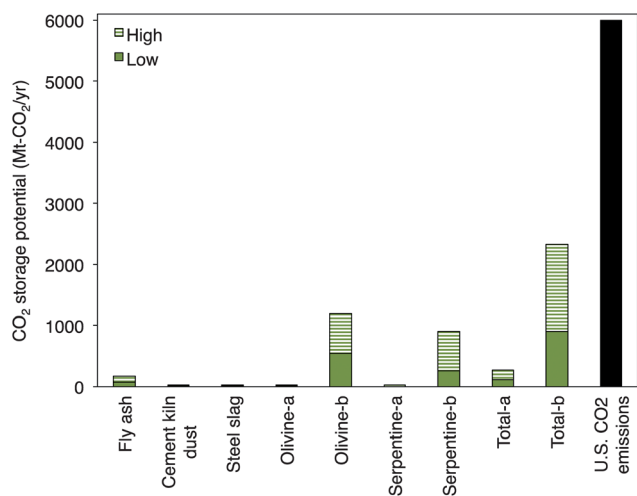


Fig. 5 Parameter sensitivity for the OI – 155 °C base case; note that for material losses during transport stages only the low, base, and high efficiency values are 5, 3, and 1%.



**Fig. 6** CO<sub>2</sub> storage potential of mineral carbonation of various alkalinity sources compared to U.S. CO<sub>2</sub> emissions; alkalinity source availability is based on U.S. production rates; for natural alkalinity sources “a” assumes a production rate of 18 Mt per year, equivalent to U.S. lime production, and “b” of 760 Mt per year, equivalent to U.S. sand and gravel production.<sup>15,42</sup>

### 3.6 Mineral carbonation potential

The CO<sub>2</sub> storage potential of mineral carbonation is estimated using the life-cycle assessment results and alkalinity source availability. Fig. 6 shows the CO<sub>2</sub> storage potential of mineral carbonation for the different alkalinity sources compared to annual U.S. CO<sub>2</sub> emissions. The annual storage potential for a given alkalinity source was calculated by multiplying its availability (Mt per year) by the CO<sub>2</sub> sequestration efficiency of mineral carbonation of that alkalinity source (t-CO<sub>2</sub>/t-alkalinity source). For industrial alkalinity sources, availability is based on U.S. production rates.<sup>37</sup> For natural alkalinity sources, availability is estimated based on U.S. production rates of (a) lime (18 Mt per year) or (b) sand and gravel (760 Mt per year).<sup>15,42</sup> The low estimate assumes the maximum sequestration efficiency of the alkalinity source obtained in the current work and the high estimate assumes a sequestration efficiency of 85%. The total CO<sub>2</sub> storage potential for the alkalinity sources considered U.S. ranges from 1.8% to 23.7% of U.S. CO<sub>2</sub> emissions, depending on the assumed availability of natural alkalinity sources and efficiency of the mineral carbonation processes.

## 4. Conclusions

The life-cycle assessment of aqueous CO<sub>2</sub> mineral carbonation technologies suggests that a variety of alkalinity sources and processes are capable of net CO<sub>2</sub> reductions. The maximum net mitigation potential was 858 t-CO<sub>2</sub> per day with CKD at ambient temperature and pressure conditions. In order of decreasing efficiency, the maximum net mitigation potentials for the other alkalinity sources investigated are: olivine, 747 t-CO<sub>2</sub> per day; SS, 656 t-CO<sub>2</sub> per day; FA, 552 t-CO<sub>2</sub> per day; and serpentine, 346 t-CO<sub>2</sub> per day.

Within the range of parameters tested, for all cases maximizing the extent reacted unambiguously improves process efficiency. In general, the maximization of the extent reacted of material is

critical to optimizing the processes because it minimizes the material handling requirements which contribute negatively to the energy budget. In particular:

- process efficiency is maximized by increasing extent reacted;
- it is critical to enhance extent reacted through most energetically favorable enhancement measure (*i.e.* increasing temperature and decreasing particle size are cheaper than increasing residence time);
- heating is the main energy driver across all non-ambient *T* processes;
- mixing and grinding are also significant energy drivers;
- reuse of carbonate as aggregate does not necessarily improve life-cycle energy efficiency (due to the tradeoff between additional separations required and offset mining emissions);
- not all alkalinity sources benefit from high reaction temperatures;
- any steps to increase reaction rates would dramatically improve process efficiency.

The total CO<sub>2</sub> storage potential for the alkalinity sources considered in the U.S. ranges from 1.3% to 23.7% of U.S. CO<sub>2</sub> emissions, depending on the assumed availability of natural alkalinity sources and efficiency of the mineral carbonation processes. To optimize a given process, building more detailed process models (*e.g.*, in ASPEN or similar chemical engineering software) would be required to better describe the reaction rates, process throughputs, required energy, and capital investment for the mineral carbonation process. Other reaction processes could be modeled, including the use of chemical additives to enhance dissolution kinetics, gas–solid reactions and low intensity mineral carbonation pathways (*e.g.*, slow ambient-temperature processes, such as lagoons at ambient temperature). Additionally, system boundaries could be extended to include capture of CO<sub>2</sub> and thereby account for the different separation and compression requirements of the various cases. Accounting for such a broad range of mineral carbonation processes within a consistent framework would allow better comparison between diverse process configurations and point to areas worthy of more detailed modeling.

## Acknowledgements

The authors acknowledge the support of the Joint Institute for Strategic Energy Analysis, which is operated by the Alliance for Sustainable Energy, LLC, on behalf of the U.S. Department of Energy’s National Renewable Energy Laboratory, the University of Colorado-Boulder, the Colorado School of Mines, the Colorado State University, the Massachusetts Institute of Technology, and Stanford University. Professor Charles F. Harvey and Dr Kurt Z. House are also acknowledged for helpful discussions.

## Notes and references

- 1 IPCC, *Special Report on Carbon Dioxide Capture and Storage*, Cambridge University Press, Cambridge, UK, 2005.
- 2 R. A. Berner, *Am. J. Sci.*, 1982, **282**, 451–473.
- 3 B. Metz, O. Davidson, H. de Coninck, M. Loos and L. Meyer, *IPCC, 2005: IPCC Special Report on Carbon dioxide Capture and Storage. Prepared by Working Group III of the International Panel on Climate Change*, Cambridge University Press, Cambridge, 2005.

- 4 K. S. Lackner, *Annual Review of Energy and the Environment*, 2002, **27**, 193–232.
- 5 S. C. Krevor, C. R. Graves, B. S. Van Gosen and A. E. McCafferty, *U.S. Geological Survey Data Series 414*, 2009.
- 6 S. J. Gerdemann, K. O. C. William, D. C. Dahlin, L. R. Penner and H. Rush, *Environ. Sci. Technol.*, 2007, **41**, 2587–2593.
- 7 S. C. M. Krevor and K. S. Lackner, *Int. J. Greenhouse Gas Control*, 2011, **5**, 1073–1080.
- 8 D. T. Van Essendelft and H. H. Schobert, *Ind. Eng. Chem. Res.*, 2009, **48**, 2556–2565.
- 9 D. N. Huntzinger, J. S. Gierke, S. K. Kawatra, T. C. Eisele and L. L. Sutter, *Environ. Sci. Technol.*, 2009, **43**, 1986–1992.
- 10 D. N. Huntzinger, J. S. Gierke, L. L. Sutter, S. K. Kawatra and T. C. Eisele, *J. Hazard. Mater.*, 2009, **168**, 31–37.
- 11 D. Bonenfant, L. Kharoune, S. Sauvé, R. Hausler, P. Niquette, M. Mimeault and M. Kharoune, *Ind. Eng. Chem. Res.*, 2008, **47**, 7610–7616.
- 12 W. J. J. Huijgen and R. N. J. Comans, *Environ. Sci. Technol.*, 2005, **39**, 9676–9682.
- 13 S. Lekakh, C. Rawlins, D. Robertson, V. Richards and K. Peaslee, *Metall. Mater. Trans. B*, 2008, **39**, 125–134.
- 14 J. K. Stolaroff, G. V. Lowry and D. W. Keith, *Energy Convers. Manage.*, 2005, **46**, 687–699.
- 15 K. E. Kelly, G. D. Silcox, A. F. Sarofim and D. W. Pershing, *Int. J. Greenhouse Gas Control*, 2011, **5**, 1587–1595.
- 16 W. J. J. Huijgen, G. J. Witkamp and R. N. J. Comans, *Chem. Eng. Sci.*, 2006, **61**, 4242–4251.
- 17 P. S. Newall, C. Consultants and I. E. A. G. G. R and D. Programme, *CO<sub>2</sub> Storage as Carbonate Minerals*, IEA Greenhouse Gas R & D Programme, Cheltenham, Gloucestershire, UK, 2000.
- 18 S. C. Krevor and K. S. Lackner, *Energy Procedia*, 2009, **1**, 4867–4871.
- 19 G. Costa, R. Baciocchi, A. Poletini, R. Pomi, C. Hills and P. Carey, *Environ. Monit. Assess.*, 2007, **135**, 55–75.
- 20 K. S. Lackner, *Annual Review of Energy and the Environment*, 2003, **27**, 193–232.
- 21 M. Mazzotti, J. C. Abanades, R. Allam, K. S. Lackner, F. Meunier, E. Rubin, J. C. Sanchez, K. Yogo and R. Zevenhoven, in *IPCC Special Report on Carbon Capture and Sequestration*, ed. B. Metz, O. Davidson, H. de Coninck, M. Loos and L. Meyer, Cambridge University Press, Cambridge, 2007.
- 22 A. L. Chaffee, G. P. Knowles, Z. Liang, J. Zhang, P. Xiao and P. A. Webley, *Int. J. Greenhouse Gas Control*, 2007, **1**, 11–18.
- 23 T. D. Kelly and G. R. Matos, in *Historical Statistics for Mineral and Material Commodities in the United States: U.S. Geological Survey Data Series 140*, ed. U. S. G. Survey, U.S. Geological Survey, 2005.
- 24 T. D. Kelly and G. R. Matos, in *Historical Statistics for Mineral and Material Commodities in the United States: U.S. Geological Survey Data Series 140*, ed. U. S. G. Survey, U.S. Geological Survey, 2005.
- 25 *Railroad Facts*, Association of American Railroads, Policy and Economics Department, 2009.
- 26 A. Gupta, D. Yan and D. S. Yan, *Mineral Processing Design and Operation: An Introduction*, Elsevier Science, 2006.
- 27 G. P. Towler and R. K. Sinnott, *Chemical Engineering Design: Principles, Practice and Economics of Plant and Process Design*, Butterworth-Heinemann, 2008.
- 28 F. P. Incropera and D. P. DeWitt, *Fundamentals of Heat and Mass Transfer*, 5th ed., John Wiley & Sons, 2002.
- 29 G. Tchobanoglous, *Wastewater Engineering: Treatment, Disposal, and Reuse*, McGraw-Hill, New York, 3rd edn, 1991.
- 30 G. B. Tatterson, *Scaleup and Design of Industrial Mixing Processes*, McGraw-Hill, 1994.
- 31 G. D. Ulrich and P. T. Vasudevan, *Chemical Engineering Process Design and Economics: A Practical Guide*, Process Pub., 2004.
- 32 A. Horvath, *Annu. Rev. Environ. Resour.*, 2004, **29**, 181–204.
- 33 M. Mikkelsen, M. Jørgensen and F. C. Krebs, *Energy Environ. Sci.*, 2010, **3**, 43–81.
- 34 A. Chizmeshya, M. McKelvy, G. Wolf, R. Carpenter and D. Gormley, *Enhancing the Atomic-Level Understanding of CO<sub>2</sub> Mineral Sequestration Mechanisms via Advanced Computational Modeling*, Arizona State University Center for Solid State Science, 2003.
- 35 G. Guthrie, J. W. Carey, D. Bergfeld, D. Byler, S. Chipera, H. J. Ziock and K. Lackner, *NETL Meeting on Carbon Capture and Sequestration*, Pittsburgh, PA, 2001.
- 36 K. Jarvis, R. Carpenter, T. Windman, Y. Kim, R. Nunez and F. Alawneh, *Environ. Sci. Technol.*, 2009, **43**, 6314–6319.
- 37 M. Back, M. Kuehn, H. Stanjek and S. Peiffer, *Environ. Sci. Technol.*, 2008, **42**, 4520–4526.
- 38 M. Hännchen, V. Prigiobbe, G. Storti, T. M. Seward and M. Mazzotti, *Geochim. Cosmochim. Acta*, 2006, **70**, 4403–4416.
- 39 J. L. Palandri and Y. K. Kharaka, *A Compilation of Rate Parameters of Water-Mineral Interaction Kinetics for Application to Geochemical Modelling*, US Geological Survey, Water-Resources Investigations Report 04-1068, 2004.
- 40 V. Prigiobbe and M. Mazzotti, Dissolution of Olivine in Presence of Oxalate, Citrate and CO<sub>2</sub> at 90°C and 120°C, *Chem. Eng. Sci.*, 2011, **66**(24), 6544–6554.
- 41 M. Hännchen, S. Krevor, M. Mazzotti and K. S. Lackner, *Chem. Eng. Sci.*, 2007, **62**, 6412–6422.
- 42 T. P. Dolley, *Sand and Gravel (Industrial) Statistics*, US Geological Survey, 2009.